Experimental Neurology 290 (2017) 95–105

Contents lists available at ScienceDirect

Experimental Neurology

journal homepage: www.elsevier.com/locate/yexnr

Research Paper

Facilitation of distinct inhibitory synaptic inputs by chemical anoxia in neurons in the oculomotor, facial and hypoglossal motor nuclei of the rat

Satoshi Takagi [a,b], Yu Kono [a,*], Masashi Nagase [b,c], Soichiro Mochio [a], Fusao Kato [b,c]

[a] Department of Neurology, The Jikei University School of Medicine, Japan
[b] Department of Neuroscience, The Jikei University School of Medicine, Japan
[c] Center for Neuroscience of Pain, The Jikei University School of Medicine, Japan

ARTICLE INFO

Article history:
Received 8 June 2016
Received in revised form 19 December 2016
Accepted 17 January 2017
Available online 19 January 2017

Keywords:
GABA
Glycine
IPSC
Patch-clamp
Sodium cyanide
Synaptic transmission

ABSTRACT

Amyotrophic lateral sclerosis (ALS) is a fatal neurodegenerative disorder characterized by the selective loss of motor neurons in the brainstem and spinal cord. Clinical studies have indicated that there is a distinct region-dependent difference in the vulnerability of motor neurons. For example, the motor neurons in the facial and hypoglossal nuclei are more susceptible to neuronal death than those in the oculomotor nucleus. To understand the mechanism underlying the differential susceptibility to cell death of the neurons in different motor nuclei, we compared the effects of chemical anoxia on the membrane currents and postsynaptic currents in different motor nuclei. The membrane currents were recorded from neurons in the oculomotor, facial and hypoglossal nuclei in brain slices of juvenile Wistar rats by using whole-cell recording in the presence of tetrodotoxin that prevents action potential-dependent synaptic transmission. NaCN consistently induced an inward current and a significant increase in the frequency of spontaneous synaptic inputs in neurons from these three nuclei. However, this increase in the synaptic input frequency was abolished by strychnine, a glycine receptor antagonist, but not by picrotoxin in neurons from the hypoglossal and facial nuclei, whereas that in neurons from the oculomotor nucleus was abolished by picrotoxin, but not by strychnine. Blocking ionotropic glutamate receptors did not significantly affect the NaCN-induced release facilitation in any of the three motor nuclei. These results suggest that anoxia selectively facilitates glycine release in the hypoglossal and facial nuclei and GABA release in the oculomotor nucleus. The region-dependent differences in the neurotransmitters involved in the anoxia-triggered release facilitation might provide a basis for the selective vulnerability of motor neurons in the neurodegeneration associated with ALS.

1. Introduction

Motor neurons innervating the skeletal muscles are more vulnerable to energy deprivation and metabolic dysfunction than the other types of neurons (Ballanyi, 2004; von Lewinski and Keller, 2005), providing an aetiological basis for the motor neuron diseases (MND), including amyotrophic lateral sclerosis (ALS). A deficiency or failure in the supply and production of the cellular energy in the brain, such as those that observed during hypoxia, anoxia, metabolic stress and mitochondrial dysfunctions (Dupuis et al., 2004), induces various types of responses in the neurons, including depolarization (Tanaka et al., 2001; Thompson et al., 2006), hyperpolarization (Trapp and Ballanyi, 1995) and an increase in the synaptic inputs (Allen and Attwell, 2004; Kono et al., 2007).

Despite recent studies that have examined the mechanisms involved in motor neuron death in these neurodegenerative diseases, why only specific groups of motor neurons are selectively vulnerable remains poorly understood. For example, in ALS patients, the oculomotor, abducens, trochlear motor neurons and the Onuf"'s nucleus are more resistant to cell death, whereas other cranial and spinal motor neurons are highly affected. These differences have been attributed to changes in calcium homeostasis between cranial motor neurons (Reiner et al., 1995; Vanselow and Keller, 2000), expression patterns of postsynaptic NMDA receptor subunits in spinocranial motor neurons (Fukaya et al., 2005; Matsuda et al., 2003; Oshima et al., 2002) and the expression ratio of glycine and $GABA_A$ receptors in different cranial motor nuclei (Lorenzo et al., 2006). We previously demonstrated that anoxia using NaCN or 95% N_2 facilitates glycine release in hypoglossal motor neurons in rat brainstem slice preparations (Kono et al., 2007). This facilitation was absent in the neurons of the neighboring dorsal nucleus of the vagus nerve that are also cholinergic neurons innervating the non-skeletal muscles, but entirely resistant in these motor neuron diseases, unlike the hypoglossal nucleus (Kono et al., 2007). In addition, the facilitation of glycine release by anoxia resulted in an increase in the NMDA receptor-mediated currents that are sensitive to the

* Corresponding author at: Department of Neurology, The Jikei University School of Medicine, 3-25-8 Nishishimbashi, Minato, Tokyo 105-8461, Japan.
E-mail address: yu1028@jikei.ac.jp (Y. Kono).

http://dx.doi.org/10.1016/j.expneurol.2017.01.007
0014-4886/

pharmacological occlusion of the glycine binding sites (Kono et al., 2007). Therefore, we examined whether the selective facilitation of glycine release in response to anoxia is also present in other motor nuclei because previous studies had suggested that the predominance of glycine receptors compared to GABA receptors is related to the vulnerability of the motor neurons to cell death (Lorenzo et al., 2006).

Therefore, we analysed the dynamic effects of anoxia on the spontaneous synaptic inputs in the facial and oculomotor neurons, in comparison to the hypoglossal motor neurons, in the brainstem slices of rats with identical age ranges and examined whether the anoxia-induced synaptic responses correlate with the ALS-vulnerability of motor neurons.

2. Material and methods

2.1. Slice preparation

The manipulation of the animals was approved by the Animal Experiment Committee at the Jikei University School of Medicine and conformed to the Guiding Principles for the Care and Use of Animals in the Field of Physiological Sciences of the Physiological Society of Japan (1998). Transverse brainstem slices from Wistar rats (10–17 days postnatal, P) were prepared as described by Shigetomi and Kato (2004) and Kono et al. (2007). Briefly, the brainstem was dissected out under anesthesia with 5% isoflurane (in 100% O_2) and secured on the cutting stage of a vibrating blade slicer (Linear Slicer PRO 7, Dosaka EM) with the caudal end facing upwards. One to two coronal slices of 400-μm thickness containing either of the bilateral oculomotor, facial or hypoglossal nucleus were cut in ice-cold "cutting" artificial cerebrospinal fluid (ACSF) composed of (in mM): 250 glycerol, 3 KCl, 0.1 $CaCl_2$, 5 $MgCl_2$, 1.25 NaH_2PO_4, 10 D-glucose, 0.4 L-ascorbic acid and 25 $NaHCO_3$ (pH = 7.4 when bubbled with 95% O_2 + 5% CO_2; osmolarity, ~310 mOsm/kg). The use of glycerol-containing medium increased the ability to obtain healthy slices with many highly viable motor neurons (Ye et al., 2006). The slices were first incubated in a holding chamber with a constant flow of "standard" ACSF composed of (in mM): 118 NaCl, 3 KCl, 1.5 $CaCl_2$, 1 $MgCl_2$, 1.2 NaH_2PO_4, 10 D-glucose and 25 $NaHCO_3$, at 37 °C for 30 to 45 min. Next, the slices were kept at room temperature (20–25 °C) in the same chamber for 0.5–5 h until recording. Each slice was transferred to a recording chamber (~0.4 ml volume) and fixed with nylon grids attached to a platinum frame. The slice was submerged in standard ACSF and continuously superfused at a rate of 3–4 ml/min.

2.2. Patch-clamp recording

Whole-cell transmembrane currents were recorded from neurons in the oculomotor, facial and hypoglossal nuclei that were visually identified under an upright microscope (BX-50WI, Olympus) with infrared differential interference contrast (IR-DIC) optics. The locations of these nuclei were confirmed by using the adjacent myelinated structures, the ventricles and the midline (see Fig. 1 for details). The use of IR-DIC optics allowed us to record from the deep structures (>100 μm) in the slice. In addition to analysing the anoxic effects in the facial and oculomotor neurons in rats at P10–17, the responses from the hypoglossal neurons that we had previously reported in rats at P16–23 (Kono et al., 2007) were re-examined in younger animals. Patch-clamp electrodes were made from borosilicate glass pipettes (1B120F-4; World Precision Instruments). The pipette solution contained (in mM): 120 CsCl, 20 TEA, 1 NaCl, 0.5 $CaCl_2$, 1 $MgCl_2$, 1 Na_2ATP, 1 BAPTA and 10 HEPES (pH 7.2, as adjusted with CsOH; osmolarity; ~310 mOsm/kg). The tip resistance of the electrode when using these solutions was 3.2–8.5 MΩ. Use of this internal solution allowed us to record the EPSCs and ISPCs as inward postsynaptic currents. The neurons we recorded consistently had the following properties: large soma size as observed with IR-DIC (>~20 μm) and small input resistance (<100 MΩ; see Table 1). Though we cannot completely rule out the possibility that some of the recordings were made from interneuron within these motor nucleus, these criteria are supportive of the notion that most of the neurons recorded are likely to be motor neurons.

The membrane currents were recorded using a MultiClamp 700B amplifier (Molecular Devices), low-pass filtered at 2 kHz and sampled at 4 kHz using a PowerLab interface (AD Instruments, CO, USA). The series resistance was 12.5 ± 1.1 MΩ ($n = 26$), 12.6 ± 0.7 MΩ ($n = 27$) and 13.4 ± 1.2 MΩ ($n = 27$) for neurons in the oculomotor, facial and hypoglossal nucleus, respectively. Whole-cell capacitance was compensated for. The resting membrane potential and input resistance (break-in resistance) was measured immediately after the cell membrane was ruptured by measuring the current response to a 5 mV (5 ms duration) command pulse, which was controlled by the Pclamp 9.0 software (Axon Instruments) (Table 1). Cells showing no overshooting action potentials upon injection of depolarising current and those showing unstable or small resting potential were discarded. After verification of the action potentials, all recordings were made in the presence of 1 μM tetrodotoxin citrate (TTX; Alomone, Israel) to block action potential-dependent transmitter release. The membrane potential was held at −70 mV during the recording. All experiments were performed at room temperature (20–25 °C).

2.3. Metabolic disturbance and drug application

Slices were treated with two types of metabolic disturbance: (i) "anoxia", application of ACSF saturated with 95% N_2 + 5% CO_2 instead of 95% O_2 + 5% CO_2 and (ii) "chemical anoxia", addition of 1 mM NaCN to the ACSF. In each slice only one neuron was recorded, and one slice was treated only once with either of the two metabolic disturbances. In addition to 1 μM TTX, 1 μM strychnine, 100 μM picrotoxin or 3 mM kynurenic acid were dissolved in the ACSF and bath-applied to selectively block glycine, $GABA_{A/C}$ or ionotropic glutamate receptors, respectively. The blockers were perfused for a minimum of 15 min before the addition of NaCN. During these experiments, the ACSF with NaCN also contained the same concentration of each blocker. Both the hypoxic ACSF and NaCN solutions were applied via a separate pipette with the outflow located near the slice, and the application was controlled with electromagnetic valves. All other compounds were purchased from Sigma-Aldrich or Nacalai Tesque (Kyoto, Japan).

2.4. Data analysis

The recorded membrane currents, including the postsynaptic currents (PSCs), were analysed off-line with an Igor Pro (WaveMetrics, OR, USA) using procedures written by one of the authors (F. K). The details of the PSC analysis are described elsewhere (Kato and Shigetomi, 2001; Shigetomi and Kato, 2004). Briefly, the action-potential independent PSCs were semi-automatically detected by calculating the co-variance function between the original trace and the template PSC waveforms. All detected synaptic events were visually confirmed so that each event had a typical PSC waveform, i.e., a rapid rise and an exponential decay. The "unlikely" PSC events and the PSC events with the peak amplitude being smaller than the basal noise level (1.96 fold of the standard deviation of the background amplitude fluctuation) were carefully discarded by visual inspection of the time-extended traces. The PSC frequency was defined as the number of PSCs occurring within a fixed time window divided by its duration (10 s for each neuron). These durations were defined empirically so that the stable and smooth time-course of the PSC frequency could be described.

In the Results section and Figures, we defined the following parameters to quantify the changes in synaptic inputs and to make statistical comparisons. (1) "PSC frequency": as defined above, the number of detected PSC events within 10-s windows and divided by 10 to give a value for events/s. This was indicated as "IPSC frequency" only when the recording was made in the presence of kynurenic acid (Fig. 3A and

B). (2) "The mean IPSC frequency" at pre-NaCN and during NaCN (Fig. 3B): "The mean PSC frequency at pre-NaCN" was calculated as the number of PSC events appearing in the period of 100 s immediately before the NaCN application and multiplied by three-fifth to give a value for "events/min". Similarly, the "mean PSC frequency during NaCN" was calculated as the number of detected PSC events in a 10-min period

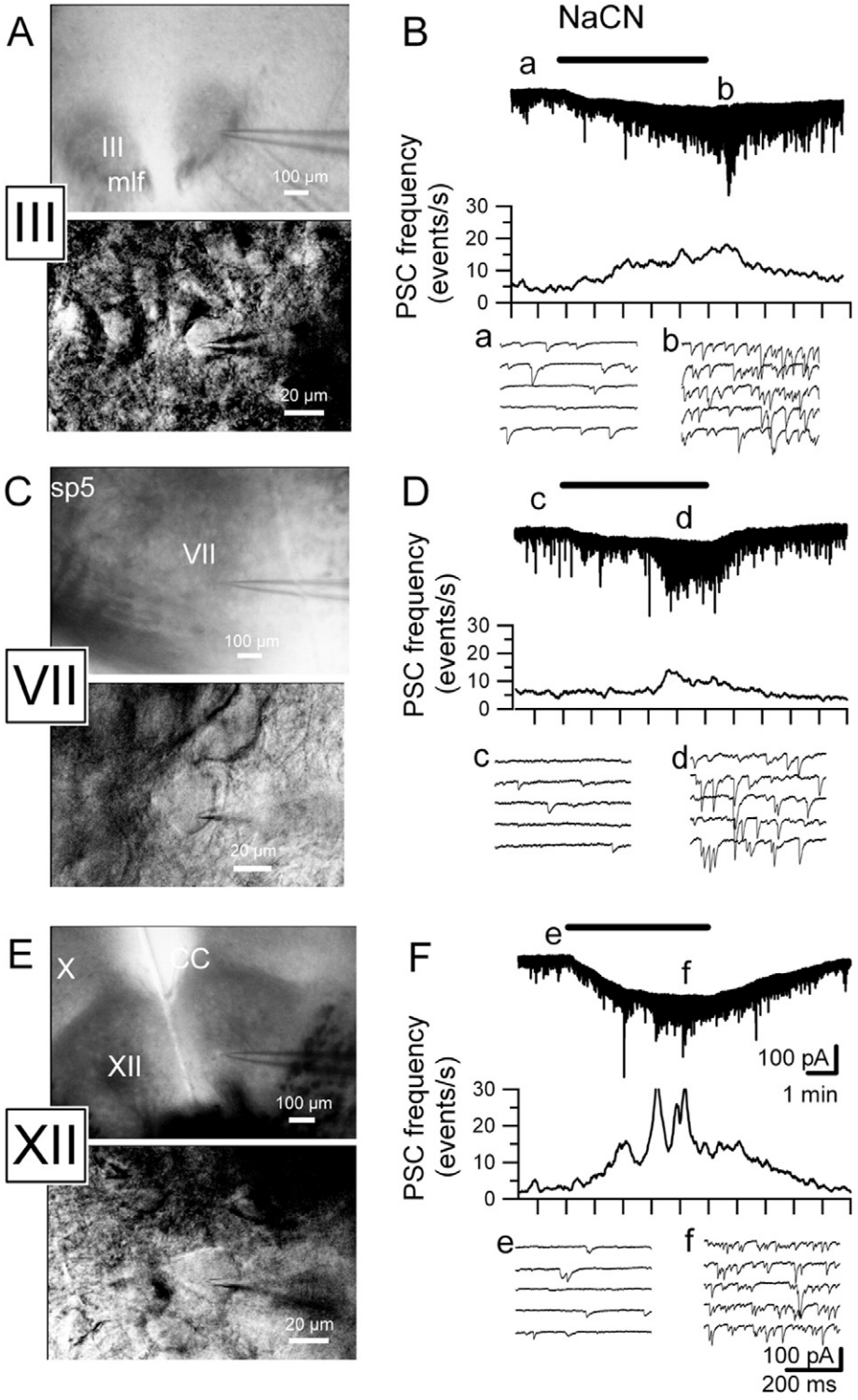

Fig. 1. NaCN generated inward currents and increased mPSC frequency in the neurons from the oculomotor, facial and hypoglossal nuclei. A. Representative micrographs of a coronal section of the rat brain including the oculomotor nucleus (upper) and the neuron being recorded in this nucleus (lower). The oculomotor nucleus is located medial to the medial longitudinal fasciculus (mlf). III, oculomotor nucleus. B. Upper: Effect of NaCN on I_m of oculomotor neurons without antagonists. NaCN (1 mM) was applied (horizontal bar) for 5 min. Middle: Time-course of the PSC frequency. Lower: Time-extended continuous recordings of the membrane currents pre-application (a) and during NaCN application (b). C. Representative micrographs of a coronal section containing the facial nucleus (upper) and the neuron being recorded in this nucleus (lower). The facial nucleus is located medial to the spinal trigeminal tract (sp5). VII, facial nucleus. D. Effect of NaCN on I_m (upper), PSC frequency (middle) and the time-extended traces (lower) of facial neurons. The upper, middle and lower panels are shown in a similar manner to B. E. Representative micrographs showing a coronal section of the rat brain including the hypoglossal nucleus (upper) and the neuron being recorded in this nucleus (lower). The hypoglossal nucleus is located ventrally to the central canal (CC). X, dorsal motor nucleus of the vagus nerve. XII, hypoglossal nucleus. F. Effect of NaCN on I_m (upper), PSC frequency (middle) and the time-extended traces (lower) of hypoglossal neurons. The upper, middle and lower panels are shown in a similar manner to B. Note the marked increase in the frequency of PSC events during application of NaCN in b, d and f for the oculomotor, facial and hypoglossal neurons, respectively.

Table 1
The membrane properties of oculomotor, facial and hypoglossal neurons.

	Age (day)	Resting potential (mV)	Input resistance (MΩ)	Cell capacitance (μF)
Oculomotor ($n = 26$)	12.5 ± 0.4	−63.2 ± 0.7	51.9 ± 2.1	89.9 ± 4.8
facial ($n = 27$)	12.0 ± 0.3	−64.2 ± 1.0	40.9 ± 3.1	118.3 ± 6.9
hypoglossal ($n = 27$)	13.0 ± 0.3	−64.8 ± 0.8	43.4 ± 3.1	99.8 ± 7.4

n, number of cells. Data are presented as mean ± S.E.M.

composed of 5 min application + 5 min gradual recovery and divided by 10 to give a value for "events/min". (3) "Increase in PSC frequency by NaCN" was calculated by dividing the mean PSC frequency during NaCN by that at pre-NaCN, and indicated as "fold increase of pre-NaCN" value. This was used only in Fig. 3B to examine if the presence of kynurenic acid affects the effect of NaCN on PSC frequency. And (4) "Maximum PSC frequency" the largest PSC frequency appearing within the 5 min application + 5 min gradual recovery period of the solution in which O_2 was replaced with N_2 (Fig. 7).

2.5. Statistical analysis

The values are expressed as mean values ± standard error of the mean (S.E.M.). The differences in the PSC frequency, PSC amplitude and the membrane properties were compared using the paired-*t*-test, Wilcoxon sign rank test and one-way ANOVA except otherwise stated. For comparisons of the effect of NaCN in the absence and presence of receptor blockers (Figs. 4, 5 and 6), two-way ANOVA was first made with before and during NaCN application and in the absence and presence of picrotoxin or strychnine, then the post-hoc comparisons were made with Holms test. Correlation between the relative change in PSC frequency and inward currents was evaluated by Spearman's rank correlation test. The differences with a probability (P) <0.05 were considered significant.

3. Results

3.1. NaCN generated inward currents and increased mPSC frequency in the oculomotor, facial and hypoglossal neurons

We recorded the transmembrane currents from the neurons of the oculomotor, facial and hypoglossal motor nuclei in transverse brain slices at different rostro-caudal levels. These motor nuclei were easily identified by their anatomical location and their view when observed with the IR-DIC optics compared to the surrounding structures, owing to the myelination of the alpha-motor axons (Fig. 1A, C, E IR-DIC) and dense segregation of the neurons with large somas (Fig. 1A, C, E IR-DIC). The resting potential, input resistance and cell capacitance are summarized in Table 1. These values were consistent with previous studies (Durand, 1989; Ikeda and Kato, 2005; Viana et al., 1994).

First, we examined the effects of "chemical anoxia" on the membrane currents in the neurons in the motor nuclei by adding NaCN, an inhibitor of complex IV (cytochrome *c* oxidase) of the mitochondrial respiratory chain, to the ACSF. Application of NaCN (1 mM) immediately generated an inward shift of the holding current (called as "inward current" hereafter). This inward current was present throughout NaCN application for each neuron group examined (5 min) and was diminished after reperfusion of the NaCN-free ACSF by 10 min in all 16 neurons examined The maximum amplitude of the inward current varied largely among neurons and between nuclei and was not statistically different between each motor neuron group (−98.0 ± 37.4 pA in the oculomotor: $n = 5$, −96.6 ± 47.3 pA in the facial: $n = 6$ and −218.3 ± 48.0 pA in the hypoglossal motor neurons: $n = 5$, one-way ANOVA).

Previously, we demonstrated that NaCN significantly increased the frequency of the spontaneous, action potential-independent and the Ca^{2+}-dependent synaptic events in the hypoglossal neurons of P16–P23 rats (Kono et al., 2007). In a similar manner to this previous report, NaCN also increased the synaptic event frequency in neurons from the oculomotor, facial nuclei (Fig. 1B and D) and hypoglossal neurons from rats at P10–17 (Fig. 1F). The time-extended versions of the membrane current traces before and during NaCN application (a-f in Fig. 1) indicate that these PSC events show typical waveforms of PSC with fast rise and exponential decay. This increase in PSC frequency lasted throughout the NaCN application (5 min) and was gradually recovered to the pre-administration level by 5 min of the post-application period in all neurons examined ($n = 5$, oculomotor; $n = 6$, facial; $n = 5$, hypoglossal neurons; the panels labelled "No Blocker" in Figs. 4A–B, 5A–B, and 6A–B). These changes in PSC frequency with NaCN were not significantly correlated with the amplitude of the maximum inward current observed in each neuron group (Spearman's rank correlation test; Fig. 2). However, when all neuron data from these three nuclei are pooled, there was a significant correlation between the change in PSC frequency and the inward current by NaCN (rho = 0.53, $p < 0.05$, Spearman's rank correlation coefficient, Fig. 2). We did not estimate the correlation between the effects of NaCN on the PSC amplitude and inward current amplitude in this study because the high-frequency occurrence of PSC during NaCN prevented us to precisely measure the baseline-to-peak amplitude.

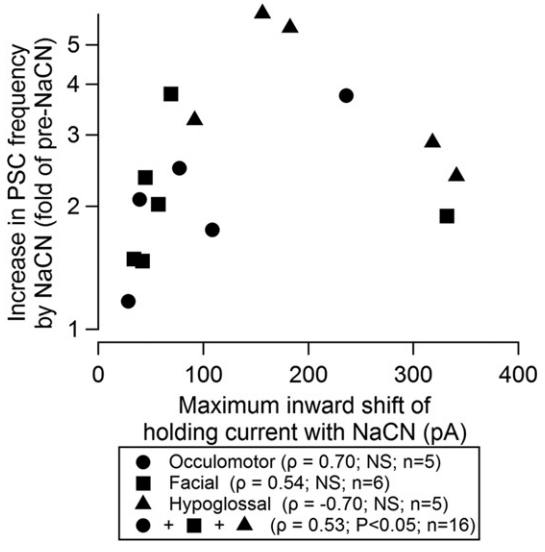

Fig. 2. Correlation between the change in maximum PSC frequency and the inward currents. Vertical axis, the increase PSC frequency by NaCN (fold increase of pre-NaCN value; log scale); horizontal axis, maximum inward shift of the holding current observed with NaCN. Filled circles, squares, and triangles present the data from oculomotor, facial and hypoglossal neurons, respectively. The values in the box show the results of Spearman's rank correlation tests.

3.2. Blockade of glutamatergic transmission did not affect the NaCN-increased facilitation of spontaneous release

We next pharmacologically identified the type of neurotransmitters and postsynaptic receptors involved in the increase in spontaneous PSC frequency with NaCN in distinct neuron groups. First, we examined whether blockade of ionotropic glutamate receptors affects the increase in spontaneous PSC frequency by analysing the effects of NaCN in the presence of kynurenic acid, a non-selective blocker of glutamate-gated receptor channels. Even in the presence of kynurenic acid (3 mM), the PSC frequency was continuously increased during and following the application of NaCN (1 mM; Fig. 3A) in neurons in the oculomotor, facial and hypoglossal motor nuclei. These effects on mean IPSC frequency (PSC is called IPSC here because these recordings were made in the continuous presence of kynurenic acid) were significant as summarized in Fig. 3B ($P < 0.05$; paired t-test; $n = 5$ for each neuron group). We also examined whether the degree of increase in PSC frequency by NaCN application is affected by the presence of kynurenic acid (Fig. 3C). In all neuron groups, application of NaCN significantly increased the PSC frequency both in the absence (open bars) and the presence (filled bars) of kynurenic acid (Wilcoxon sign rank test; $P < 0.05$). In addition, the degree of increase, as expressed by the relative PSC frequency as expressed as fold increase of the pre-NaCN value, was not significantly different between those recorded in the absence and in the presence of kynurenic acid (one-way ANOVA; $P > 0.05$; note that NaCN application was made only once in a slice and accordingly that the neuron populations for the experiments with and without kynurenic acid are distinct). These results suggest that the increase in PSC frequency by NaCN did not result

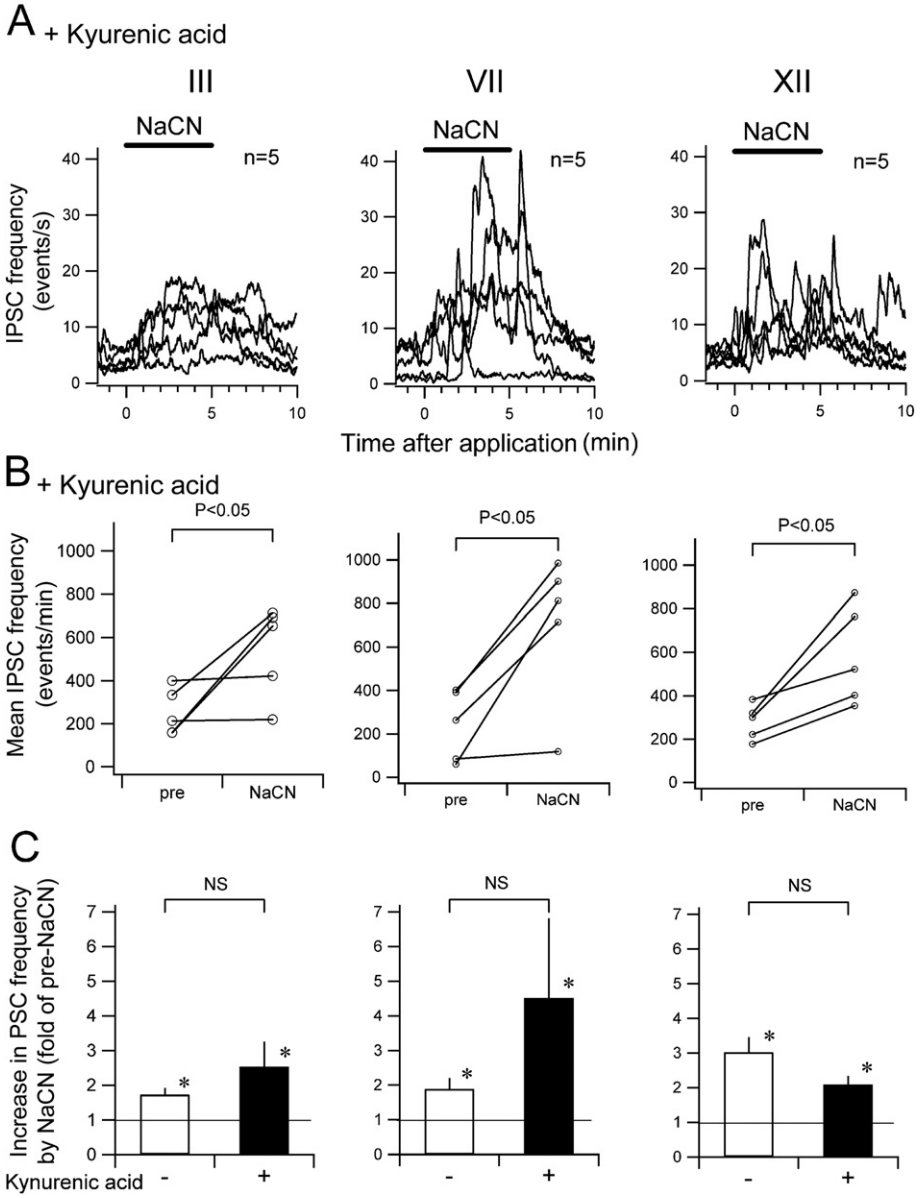

Fig. 3. Increase in PSC frequency with NaCN in the presence of kynurenic acid. A. Time-courses of the PSC frequency recorded in the presence of kynurenic acid (3 mM). NaCN (1 mM) was applied at the horizontal bar for 5 min. Overlay of the recordings in 5 neurons for each nucleus (III, oculomotor, VII, facial and XII, hypoglossal motor nucleus, respectively). B. The change in the Mean PSC frequency before NaCN application (pre; estimated for a 100-s period immediately before the application of NaCN) and that during NaCN (NaCN; estimated for a 10-min period starting from the onset of application of NaCN). PSCs were recorded in the presence of kynurenic acid (3 mM). Lines between markers indicate that the linked values are from the same neurons. Statistical comparisons were made with paired t-test. C. The NaCN effect was tested in the absence and presence of kynurenic acid ("−" and "+", respectively). The increase in mean PSC frequency during NaCN application as expressed as fold increase of the pre-NaCN value for both groups. *, significant increase in PSC frequency with NaCN vs. pre-NaCN (Wilcoxon sign rank test; $P < 0.05$). Between-group comparisons (in the presence versus in the absence of kynurenic acid) were made using one-way ANOVA (NS, $P > 0.05$; $n = 5$ for each neuron groups).

primarily from facilitated glutamate release but rather from facilitated release of inhibitory transmitters in these three groups of neurons

3.3. NaCN facilitated glycine release in facial and hypoglossal neurons

The increase in the IPSC frequency in response to NaCN and anoxia is abolished by strychnine but not by picrotoxin in the hypoglossal neurons (Kono et al., 2007). To determine whether this occurs in the facial and oculomotor neurons, we analysed the effects of blocking either $GABA_A$ receptors or glycine receptors on the NaCN-induced increase in the PSC frequency. The increase in PSC frequency in response to NaCN application was abolished by strychnine (1 μM) but not by picrotoxin (100 μM) in the facial (Fig. 5A, B, middle) and the hypoglossal neurons (Fig. 4A, B, middle). In these neuron groups, strychnine and picrotoxin did not significantly affect the mean PSC frequency observed before NaCN

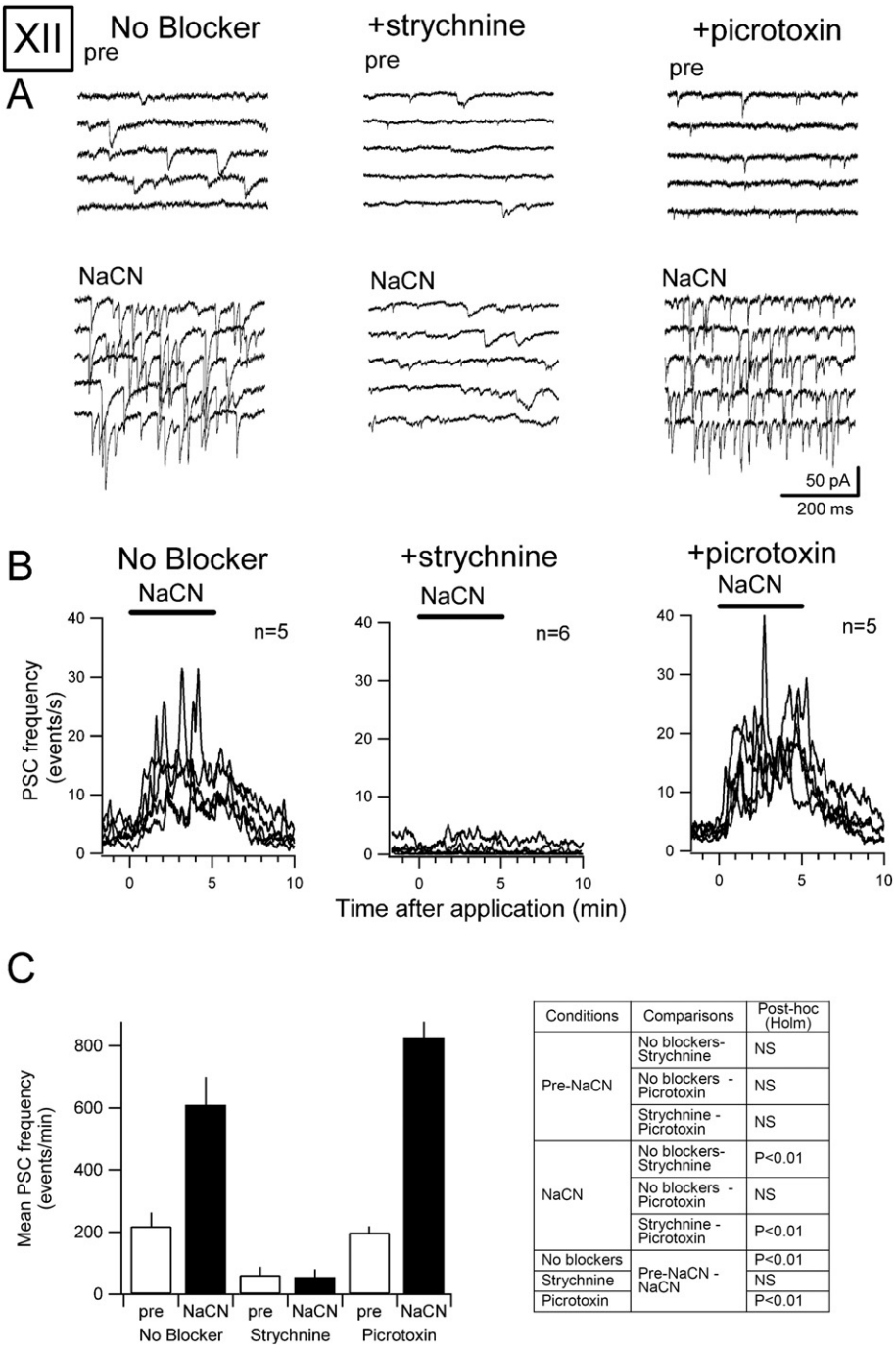

Conditions	Comparisons	Post-hoc (Holm)
Pre-NaCN	No blockers-Strychnine	NS
	No blockers - Picrotoxin	NS
	Strychnine - Picrotoxin	NS
NaCN	No blockers-Strychnine	P<0.01
	No blockers - Picrotoxin	NS
	Strychnine - Picrotoxin	P<0.01
No blockers	Pre-NaCN - NaCN	P<0.01
Strychnine		NS
Picrotoxin		P<0.01

Fig. 4. Strychnine, but not picrotoxin, suppressed the increase in the PSC frequency induced by NaCN in hypoglossal neurons. A. Time-extended traces of the continuous recordings of the membrane currents. No Blocker, recording in the absence of blockers; + strychnine, in the presence of strychnine; + picrotoxin, in the presence of picrotoxin. These three recordings are from three different neurons recorded from different slices. Pre, pre-application of NaCN (upper traces); NaCN, during NaCN application (bottom traces). Note the almost complete absence of the NaCN effect in the presence of strychnine. B. Superimposed time-course of the PSC frequency. The NaCN (1 mM) was applied (horizontal bar) for 5 min. Note the absence of the increase in frequency in the presence of strychnine. C. The effects of the receptor blockers on mean PSC frequency during NaCN in the absence and presence of blockers. No Blocker, in the absence of blockers ($n = 5$); Strychnine, in the presence of strychnine ($n = 6$); Picrotoxin, in the presence of picrotoxin ($n = 5$). "pre", mean PSC frequency for 100 s measured before NaCN application; "NaCN", that for 600 s (10 min) during and after NaCN application. Summary on the right shows the results of post-hoc analyses between all meaningful pairs (Holm test), which were performed following two-way ANOVA. NS, $P > 0.05$.

application (Figs. 4C and 5C). NaCN significantly increased the mean PSC frequency in the absence of any blockers and also in the presence of picrotoxin but not in the presence of strychnine (Figs. 4C and 5C). There was no significant difference between the mean PSC frequencies during NaCN in the absence and presence of picrotoxin but it became significantly smaller in the presence of strychnine (Figs. 4C and 5C). In contrast, picrotoxin (100 μM) did not significantly affect the increase in mean PSC frequency with NaCN in the facial and hypoglossal neurons (Figs. 4C and 5C). These results suggest that NaCN facilitates the spontaneous release of glycine, which activates strychnine-sensitive postsynaptic glycine receptors in the hypoglossal and facial neurons.

3.4. NaCN facilitated GABA release in neurons oculomotor nucleus

In contrast to the facial and hypoglossal neurons, the addition of strychnine did not significantly affect the mean PSC frequency observed before the NaCN application and also NaCN-induced

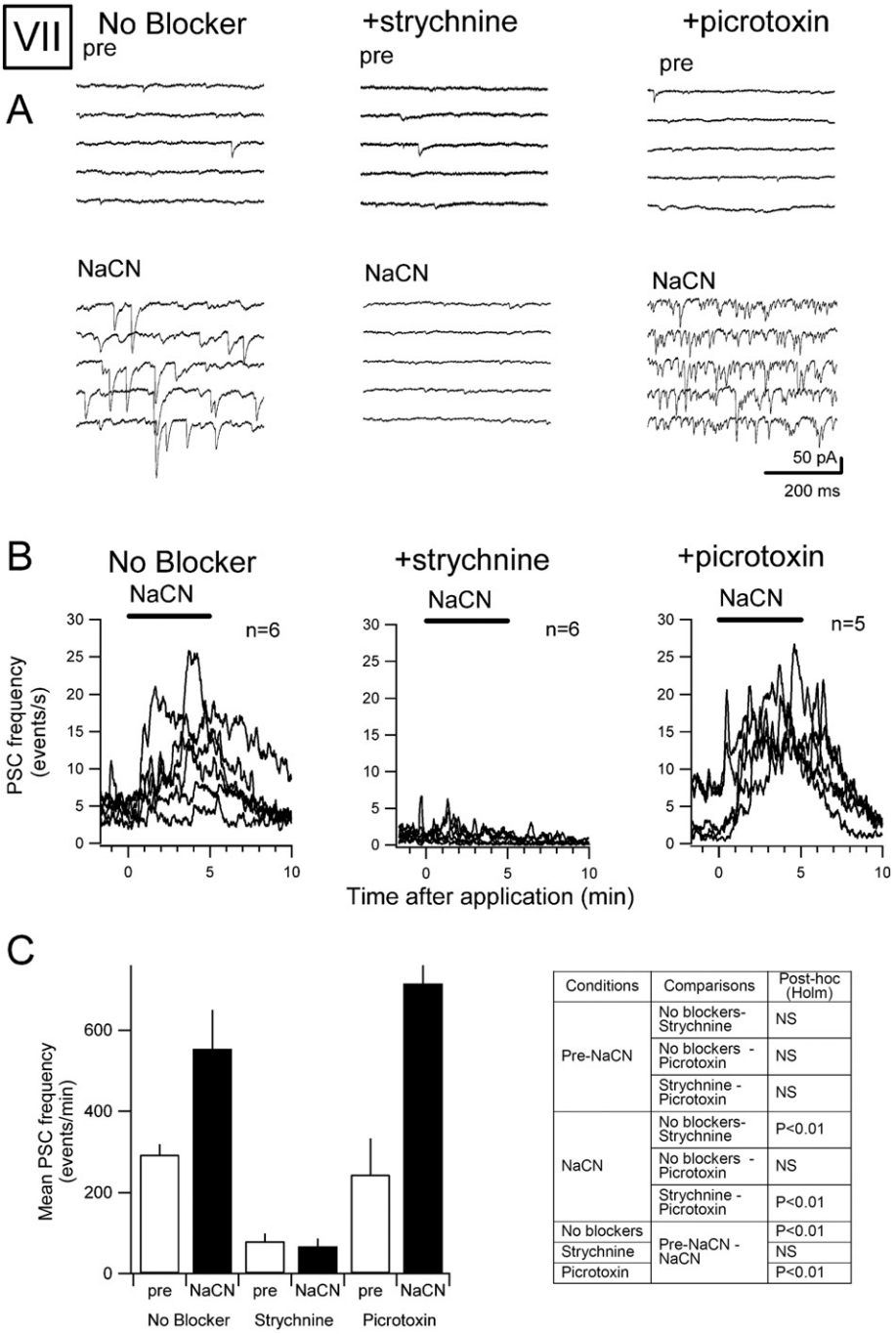

Conditions	Comparisons	Post-hoc (Holm)
Pre-NaCN	No blockers-Strychnine	NS
	No blockers - Picrotoxin	NS
	Strychnine - Picrotoxin	NS
NaCN	No blockers-Strychnine	P<0.01
	No blockers - Picrotoxin	NS
	Strychnine - Picrotoxin	P<0.01
No blockers	Pre-NaCN - NaCN	P<0.01
Strychnine		NS
Picrotoxin		P<0.01

Fig. 5. Strychnine, but not picrotoxin, suppressed the increase in the PSC frequency induced by NaCN in facial neurons. A. Time-extended traces of the continuous recordings of the membrane currents. B. Superimposed time-course of the PSC frequency. C. The effects of the receptor blockers on mean PSC frequency during NaCN in the absence and presence of blockers. No Blocker, in the absence of blockers ($n = 5$); Strychnine, in the presence of strychnine ($n = 6$); Picrotoxin, in the presence of picrotoxin ($n = 5$). "pre", mean PSC frequency for 100 s measured before NaCN application; "NaCN", that for 600 s (10 min) during and after NaCN application. Summary on the right shows the results of post-hoc analyses between all meaningful pairs (Holm test), which were performed following two-way ANOVA. NS, $P > 0.05$.

increase in the mean PSC frequency recorded in the oculomotor neurons (Fig. 6A, B, middle). However, in the oculomotor neurons, the addition of picrotoxin almost abolished the significant increase by NaCN in the PSC frequency (Fig. 6A, B, right). In the presence of picrotoxin, NaCN did not significantly increase the mean PSC frequency, while NaCN significantly increased it in the presence of strychnine, in a similar manner to that in the absence of blockers (Fig. 6C). These results strongly suggest that the increase in PSC frequency by NaCN in the oculomotor neurons is a result of the facilitation of GABA release, which contrasts the hypoglossal and facial neurons.

3.5. Elimination of extracellular O_2 facilitated release in a similar manner to chemical anoxia

We then examined whether the facilitation of glycine or GABA release in response to chemical anoxia with NaCN also occurs with "actual" anoxia by perfusing ACSF saturated with 95% N_2. Anoxia generated

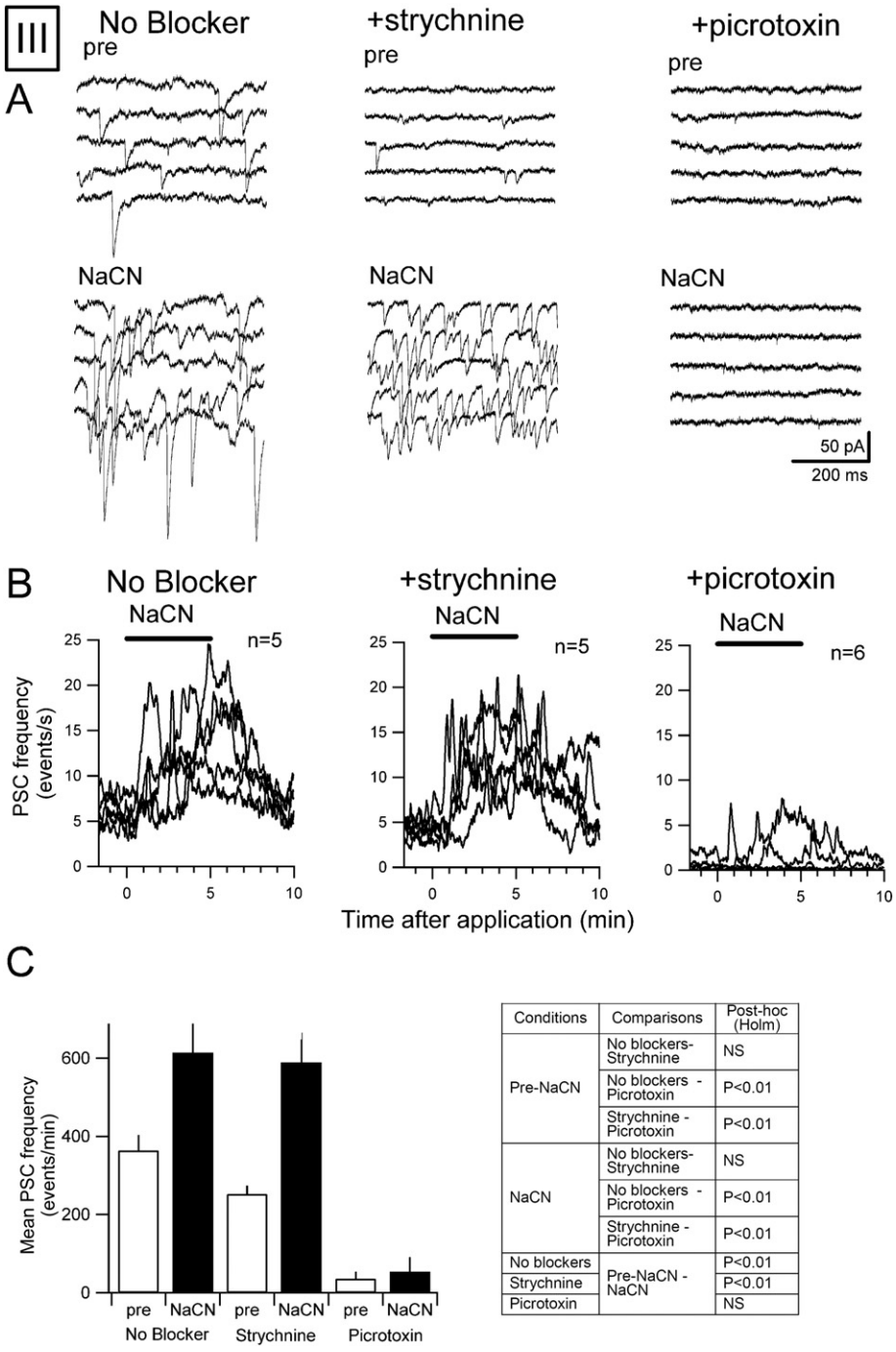

Conditions	Comparisons	Post-hoc (Holm)
Pre-NaCN	No blockers-Strychnine	NS
	No blockers - Picrotoxin	P<0.01
	Strychnine - Picrotoxin	P<0.01
NaCN	No blockers-Strychnine	NS
	No blockers - Picrotoxin	P<0.01
	Strychnine - Picrotoxin	P<0.01
No blockers	Pre-NaCN - NaCN	P<0.01
Strychnine		P<0.01
Picrotoxin		NS

Fig. 6. Picrotoxin, but not strychnine, suppressed the increase in the PSC frequency induced by NaCN in oculomotor neurons. A. Time-extended traces of the continuous recordings of the membrane currents. B. Superimposed time-course of the PSC frequency. C. The effects of the receptor blockers on mean PSC frequency during NaCN in the absence and presence of blockers. No Blocker, in the absence of blockers ($n = 5$); Strychnine, in the presence of strychnine ($n = 5$); Picrotoxin, in the presence of picrotoxin ($n = 5$). "pre", mean PSC frequency for 100 s measured before NaCN application; "NaCN", that for 600 s (10 min) during and after NaCN application. Summary on the right shows the results of post-hoc analyses between all meaningful pairs (Holm test), which were performed following two-way ANOVA. NS, $P > 0.05$.

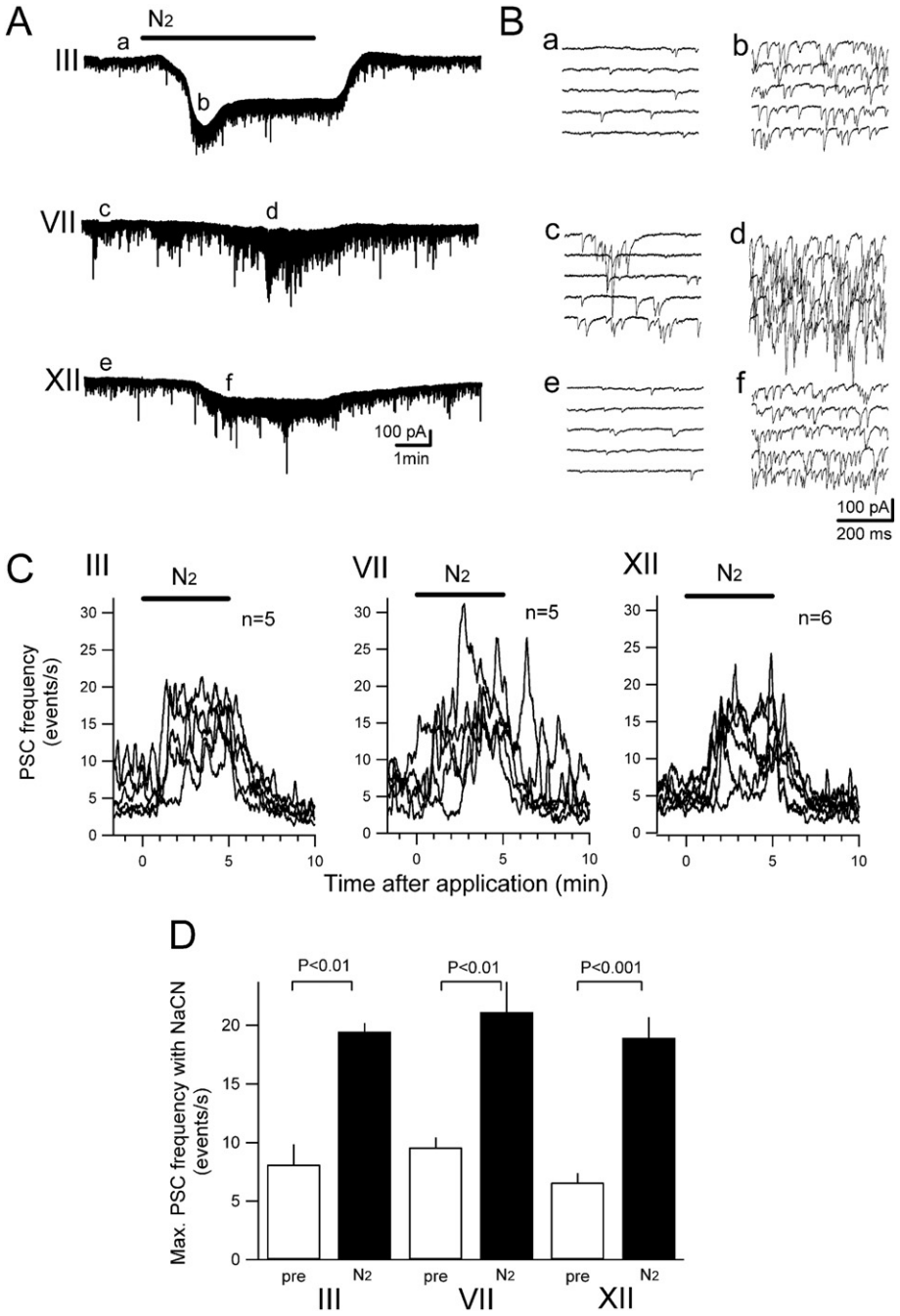

Fig. 7. Effects of anoxia on the membrane and synaptic currents in the oculomotor, facial and hypoglossal neurons. A. The effect of anoxia on I_m of the oculomotor, facial and hypoglossal neurons in the absence of antagonists. N_2 (95%) was applied (horizontal bar) for 5 min. B. Time-extended continuous recordings of the membrane currents at pre-application (*a,c,e*) and during NaCN application (*b,d,f*). Note the significant and consistent increase in the number of PSC events in *b,d and f*. C. Superimposed time-course of the PSC frequency. N_2 (95%) was applied (horizontal bar) for 5 min. Note the marked increase in the frequency of PSC events. D. Summary of the effects of anoxia on the maximum PSC frequency observed during the application of N_2 solution. Pre, pre-application of N_2; N_2, during N_2. Oculomotor neurons, $n = 5$; facial neurons, $n = 5$; hypoglossal neurons, $n = 6$; *P* values indicate the results of one-way ANOVA for each neuron group.

large inward currents (Fig. 7A, -333.8 ± 68.1 pA in the oculomotor: $n = 5$, -325.5 ± 239.3 pA in the facial: $n = 5$ and -83.1 ± 19.8 pA in hypoglossal neurons: $n = 6$) and markedly and significantly increased the frequency of PSC events (Fig. 7B). The burst-like increase in PSC frequency was observed in all neurons examined from distinct motor nucleus (Fig. 7C). The maximum PSC frequency during anoxia was significantly higher than that before anoxia (Fig. 7D). These results confirmed that the metabolic disturbances through different mechanisms and origins facilitate action potential-independent release of neurotransmitters to the neurons in different nuclei.

4. Discussion

In this study, we demonstrated that hypoxia and anoxia facilitate the action potential-independent spontaneous release of neurotransmitters with an inward shift in the holding current of the facial and oculomotor neurons, in a very similar manner to the hypoglossal neurons (Kono et al., 2007). However, the present study also demonstrated a striking difference between distinct types of neurons in the type of neurotransmitter involved in the anoxia-induced facilitation of release. In the hypoglossal and facial neurons, hypoxia almost exclusively facilitated

glycine-mediated transmission, whereas in oculomotor neurons, it facilitated GABA-mediated transmission. These findings are of particular interest because it has been indicated that these motor neurons show different vulnerabilities in neurodegenerative diseases, such as ALS; the hypoglossal and facial motor neurons are highly vulnerable, whereas the oculomotor neurons are resistant. The present findings would help understand the mechanism underlying the selective motor neuron damage that occurs during the progress of ALS.

4.1. Consequences of glycine- and GABA-mediated inhibitory transmission

Glycine and GABA are the two major inhibitory neurotransmitters in the mammalian central nervous system, activating glycine and $GABA_{A/C}$ receptors, respectively. These subsynaptic ligand-gated channels, when activated by these endogenous ligands, become permeable exclusively to Cl^- and reduces neuronal excitability through hyperpolarisation and/or reduction of the input resistance by membrane "shunting". In addition, the inhibitory synaptic transmissions mediated by GABA and glycine share common molecules, including the vesicular transporters (Ottersen et al., 1987; Taal and Holstege, 1994) in the presynaptic terminals (called as vesicular GABA transporters, VGAT or vesicular inhibitory amino acid transporters, VIAAT) and scaffolding proteins, gephryn, in the postsynaptic elements (Thompson et al., 2006).

However, the postsynaptic current of $GABA_A$ receptor channels shows slower decay kinetics than that of glycine receptors (Baccei and Fitzgerald, 2004; Gao et al., 2001; Inquimbert et al., 2007; Keller et al., 2001), enabling them to inhibit postsynaptic neurons for a longer duration. This might make the glycine-mediated inhibition weaker than that by GABA in reducing the postsynaptic excitability. In addition to the fast current kinetics of glycine receptors that limits the duration of Cl^- flow and the lack of metabotropic receptors for glycine, glycine could become pro-excitatory, depending on the situation, through activating NMDA receptors by binding to the glycine-binding site (Kono et al., 2007). For example, the genetic suppression of the glycine transporter in the forebrain results in an improved cognitive function by potentiating the NMDA receptor-mediated postsynaptic currents in mice (Yee et al., 2006). Inhibition of the glycine transporter in the hypoglossal motor neurons potentiated NMDA receptor-mediated neurotransmission (Lim et al., 2004). In neurons expressing NMDA receptors containing NR3B subunits, glycine, but not glutamate or D-serine, directly activates these receptors (Chatterton et al., 2002), which are selectively expressed in motor neurons in the trigeminal, facial, glossopharyngeal nucleus and spinal ventral horn but not in oculomotor and Onuf's nucleus (Nishi et al., 2001). In addition to the potentiation of NMDA receptor-mediated currents by synaptically released glycine during chemical hypoxia in the hypoglossal neurons (Kono et al., 2007), it has also been demonstrated that application of glycine to the cerebral cortex leads to oxidative stress and mitochondrial dysfunction in neurons, which might underlie the neurological damage in patients with hyperglycaemia (Busanello et al., 2010; Leipnitz et al., 2009). These lines of evidence support a notion that an aberrant increase in release and/or extracellular accumulation of glycine might have deteriorating influence on the neurons through direct or indirect mechanisms.

4.2. Selective release facilitation of GABA and glycine

The mechanism underlying the differential modulation by chemical anoxia of the frequency of release of GABA and glycine between distinct neuron groups is not identified. In this study, this selective release facilitation was observed in the presence of TTX, ruling out a possibility that it resulted from the difference in the anoxia-induced neuronal excitation between glycinergic and GABAergic presynaptic neurons forming synapses with neurons in distinct motor nuclei. In addition, as GABA-mediated IPSCs in hypoglossal and facial neurons, as well as glycine-mediated IPSCs in the oculomotor neurons could be clearly observed in the normoxic conditions (Figs. 4, 5 and 6), it is unlikely that glycine-mediated inputs are prevailing for the neurons in the hypoglossal and facial nuclei and also it is unlikely that GABA-mediated inputs are prevailing in the oculomotor neurons. As the conclusion above of transmitter-specific activation by NaCN was drawn on the basis of pharmacological observations, it is noteworthy that picrotoxin can block homomeric glycine receptors composed of α subunits at an IC50 of 25 μM (Chattipakorn and McMahon, 2002). However, firstly because heteromerization of α and β subunits is necessary for gephrin binding and subsequent synaptic clustering for glycine receptors (Kirsch et al., 1993; Meyer et al., 1995) and secondly because strychnine at 1 μM should almost completely suppress the α homomeric glycine receptors, if they exist, it is unlikely that the NaCN-induced PSCs blocked by picrotoxin but not by strychnine (Fig. 6) were mediated by picrotoxin-sensitive non-synaptic glycine receptors.

It is well known that the VIAAT can accumulate both glycine and GABA into the synaptic vesicles. Furthermore, in previous study, we indicated that facilitation of glycine by NaCN depends on Ca^{2+} entry though activated voltage-dependent Ca^{2+} channels (Kono et al., 2007). Therefore, the most straightforward interpretation would be that the difference in the type of transmitter of which the release was facilitated by anoxia would be due to the difference in the predominant transmitters in the anoxia-excited terminals. In motoneurons in the spinal cord and brain stem as well as sensory-associated neurons in the dorsal horn, three types of miniature IPSCs have been documented; that are those mediated exclusively by glycine receptors, those by $GABA_A$ receptors and those by both glycine and $GABA_A$ receptors (mixed type) (Keller et al., 2001; Jonas et al., 1998; O'Brien and Berger, 1999). The proportion of these three types depends on the regions and it changes in the course of development, presumably depending on the postsynaptic specification of the receptors (Keller et al., 2001; Jonas et al., 1998). The presynaptic specification between GABAergic and glycinergic terminals also seems to occur at later stage with selective expression of glutamic acid dehydrogenase (GAD), an enzyme underlying conversion from glutamate to GABA, and also that of glycine transporter type 2, which underlies selective uptake of glycine from the synaptic cleft to glycinergic neurons (Aubrey et al., 2007). In neurons without GAD protein expression, VIAATs only accumulate glycine and terminal excitation of such neurons would result in exclusive release of glycine. In addition, selective reuptake of glycine by GlyT2 would increase the glycine concentration at the terminals and subsequently its intra-vesicular concentration in these "glycinergic" terminals. In such situations, it might be possible that the postsynaptic neurons predominantly express glycine receptors at these synapses. As such, in the hypoglossal and facial nuclei, glycine, rather than GABA, would be selectively released from the anoxia-excited terminals, which is not the case for the oculomotor nucleus. In addition, it remains to be determined in the future studies 1) what is the molecular and cellular mechanism underlying such release facilitation in response to anoxia (Kono et al., 2007), 2) if such mechanism could be identified, how is the expression of such mechanism associated with the glycinergic phenotype without GAD expression and with GlyT2 expression, and 3) why such mechanism is not expressed for the terminals releasing glutamate, that is also another prevailing neurotransmitter to the motor neurons.

4.3. Difference in the motoneuron vulnerability in ALS

A number of studies have clarified differences in various properties between different cranial and spinal motor neurons in aiming to account for the well-described differences in the vulnerability in motor neurons diseases such as the ALS. While the trigeminal, facial and hypoglossal neurons are vulnerable, the oculomotor, trochlear and abducens neurons are relatively resistant, defining the typical progress of the ALS-associated symptoms. Various types of differences in the properties of these motor neurons have been proposed to account for their distinct vulnerability (Chatterton et al., 2002; Fukaya et al., 2005; Fuller et al., 2006; Haenggeli and Kato, 2002; Hayashi et al., 1981; Lorenzo et al.,

2006; Martin and Chang, 2012; Matsuda et al., 2003; Nishi et al., 2001; Oshima et al., 2002). Our present findings of a larger fraction of glycinergic inputs and their selective facilitation in response to anoxia in the neurons from ALS-vulnerable nuclei add another property that would distinguish the fate of neurons under pathological loads. The causal relationship between the type postsynaptic receptors activated by metabolic stress-induced release of specific type of transmitters and the neuronal vulnerability should be clarified in the future study.

Acknowledgments

This work was supported, in part, by Grants-in-Aid from the Ministry of Education, Culture, Sports, Science and Technology, Japan (Nos. 21390436 to F.K. and 18790604 to Y.K.) and Grants for the Research on Health Sciences focusing on Drug Innovation from The Japan Health Sciences Foundation (KH21006) to F.K. We thank Y. Takahashi for critical reading of the manuscript and T. Matsuo-Tarumi for technical assistance during preparation of the manuscript.

References

Allen, N.J., Attwell, D., 2004. The effect of simulated ischaemia on spontaneous GABA release in area CA1 of the juvenile rat hippocampus. J. Physiol. 561, 485–498.
Aubrey, K.R., Rossi, F.M., Ruivo, R., Alboni, S., Bellenchi, G.C., Le Goff, A., Gasnier, B., Supplisson, S., 2007. The transporters GlyT2 and VIAAT cooperate to determine the vesicular glycinergic phenotype. J. Neurosci. 27, 6273–6281.
Baccei, M.L., Fitzgerald, M., 2004. Development of GABAergic and glycinergic transmission in the neonatal rat dorsal horn. J. Neurosci. 24, 4749–4757.
Ballanyi, K., 2004. Protective role of neuronal KATP channels in brain hypoxia. J. Exp. Biol. 207, 3201–3212.
Busanello, E.N., Moura, A.P., Viegas, C.M., Zanatta, A., da Costa Ferreira, G., Schuck, P.F., Wajner, M., 2010. Neurochemical evidence that glycine induces bioenergetical dysfunction. Neurochem. Int. 56, 948–954.
Chatterton, J.E., Awobuluyi, M., Premkumar, L.S., Takahashi, H., Talantova, M., Shin, Y., Cui, J., Tu, S., Sevarino, K.A., Nakanishi, N., Tong, G., Lipton, S.A., Zhang, D., 2002. Excitatory glycine receptors containing the NR3 family of NMDA receptor subunits. Nature 415, 793–798.
Chattipakorn, S.C., McMahon, L.L., 2002. Pharmacological characterization of glycine-gated chloride currents recorded in rat hippocampal slices. J. Neurophysiol. 87, 1515–1525.
Dupuis, L., Gonzalez de Aguilar, J.L., Oudart, H., de Tapia, M., Barbeito, L., Loeffler, J.P., 2004. Mitochondria in amyotrophic lateral sclerosis: a trigger and a target. Neurodegener. Dis. 1, 245–254.
Durand, J., 1989. Intracellular study of oculomotor neurons in the rat. Neuroscience 30, 639–649.
Fukaya, M., Hayashi, Y., Watanabe, M., 2005. NR2 to NR3B subunit switchover of NMDA receptors in early postnatal motoneurons. Eur. J. Neurosci. 21, 1432–1436.
Fuller, P.I., Reddrop, C., Rodger, J., Bellingham, M.C., Phillips, J.K., 2006. Differential expression of the NMDA NR2B receptor subunit in motoneuron populations susceptible and resistant to amyotrophic lateral sclerosis. Neurosci. Lett. 399, 157–161.
Gao, B.X., Stricker, C., Ziskind-Conhaim, L., 2001. Transition from GABAergic to glycinergic synaptic transmission in newly formed spinal networks. J. Neurophysiol. 86, 492–502.
Haenggeli, C., Kato, A.C., 2002. Differential vulnerability of cranial motoneurons in mouse models with motor neuron degeneration. Neurosci. Lett. 335, 39–43.
Hayashi, H., Suga, M., Satake, M., Tsubaki, T., 1981. Reduced glycine receptor in the spinal cord in amyotrophic lateral sclerosis. Ann. Neurol. 9, 292–294.
Ikeda, R., Kato, F., 2005. Early and transient increase in spontaneous synaptic inputs to the rat facial motoneurons after axotomy in isolated brainstem slices of rats. Neuroscience 134, 889–899.
Inquimbert, P., Rodeau, J.L., Schlichter, R., 2007. Differential contribution of GABAergic and glycinergic components to inhibitory synaptic transmission in lamina II and laminae III-IV of the young rat spinal cord. Eur. J. Neurosci. 26, 2940–2949.
Jonas, P., Bischofberger, J., Sandkuhler, J., 1998. Corelease of two fast neurotransmitters at a central synapse. Science 281, 419–424.
Kato, F., Shigetomi, E., 2001. Distinct modulation of evoked and spontaneous EPSCs by purinoceptors in the nucleus tractus solitarii of the rat. J. Physiol. 530, 469–486.
Keller, A.F., Coull, J.A., Chery, N., Poisbeau, P., De Koninck, Y., 2001. Region-specific developmental specialization of GABA-glycine cosynapses in laminas I-II of the rat spinal dorsal horn. J. Neurosci. 21, 7871–7880.
Kirsch, J., Wolters, I., Triller, A., Betz, H., 1993. Gephyrin antisense oligonucleotides prevent glycine receptor clustering in spinal neurons. Nature 6457, 745–748.
Kono, Y., Shigetomi, E., Inoue, K., Kato, F., 2007. Facilitation of spontaneous glycine release by anoxia potentiates NMDA receptor current in the hypoglossal motor neurons of the rat. Eur. J. Neurosci. 25, 1748–1756.
Leipnitz, G., Solano, A.F., Seminotti, B., Amaral, A.U., Fernandes, C.G., Beskow, A.P., Dutra Filho, C.S., Wajner, M., 2009. Glycine provokes lipid oxidative damage and reduces the antioxidant defenses in brain cortex of young rats. Cell. Mol. Neurobiol. 29, 253–261.
Lim, R., Hoang, P., Berger, A.J., 2004. Blockade of glycine transporter-1 (GLYT-1) potentiates NMDA receptor-mediated synaptic transmission in hypoglossal motorneurons. J. Neurophysiol. 92, 2530–2537.
Lorenzo, L.E., Barbe, A., Portalier, P., Fritschy, J.M., Bras, H., 2006. Differential expression of GABAA and glycine receptors in ALS-resistant vs. ALS-vulnerable motoneurons: possible implications for selective vulnerability of motoneurons. Eur. J. Neurosci. 23, 3161–3170.
Martin, L.J., Chang, Q., 2012. Inhibitory synaptic regulation of motoneurons: a new target of disease mechanisms in amyotrophic lateral sclerosis. Mol. Neurobiol. 45, 30–42.
Matsuda, K., Fletcher, M., Kamiya, Y., Yuzaki, M., 2003. Specific assembly with the NMDA receptor 3B subunit controls surface expression and calcium permeability of NMDA receptors. J. Neurosci. 23, 10064–10073.
Meyer, G., Kirsch, J., Betz, H., Langosch, D., 1995. Identification of a gephyrin binding motif on the glycine receptor beta subunit. Neuron 15, 563–572.
Nishi, M., Hinds, H., Lu, H.P., Kawata, M., Hayashi, Y., 2001. Motoneuron-specific expression of NR3B, a novel NMDA-type glutamate receptor subunit that works in a dominant-negative manner. J. Neurosci. 21, RC185.
O'Brien, J.A., Berger, A.J., 1999. Cotransmission of GABA and glycine to brain stem motoneurons. J. Neurophysiol. 82, 1638–1641.
Oshima, S., Fukaya, M., Masabumi, N., Shirakawa, T., Oguchi, H., Watanabe, M., 2002. Early onset of NMDA receptor GluR epsilon 1 (NR2A) expression and its abundant postsynaptic localization in developing motoneurons of the mouse hypoglossal nucleus. Neurosci. Res. 43, 239–250.
Ottersen, O.P., Davanger, S., Storm-Mathisen, J., 1987. Glycine-like immunoreactivity in the cerebellum of rat and Senegalese baboon, *Papio papio*: a comparison with the distribution of GABA-like immunoreactivity and with [3*H*]glycine and [3*H*]GABA uptake. Exp. Brain Res. 66, 211–221.
Reiner, A., Medina, L., Figueredo-Cardenas, G., Anfinson, S., 1995. Brainstem motoneuron pools that are selectively resistant in amyotrophic lateral sclerosis are preferentially enriched in parvalbumin: evidence from monkey brainstem for a calcium-mediated mechanism in sporadic ALS. Exp. Neurol. 131, 239–250.
Shigetomi, E., Kato, F., 2004. Action potential-independent release of glutamate by Ca2 + entry through presynaptic P2X receptors elicits postsynaptic firing in the brainstem autonomic network. J. Neurosci. 24, 3125–3135.
Taal, W., Holstege, J.C., 1994. GABA and glycine frequently colocalize in terminals on cat spinal motoneurons. Neuroreport 5, 2225–2228.
Tanaka, E., Yasumoto, S., Hattori, G., Niiyama, S., Matsuyama, S., Higashi, H., 2001. Mechanisms underlying the depression of evoked fast EPSCs following in vitro ischemia in rat hippocampal CA1 neurons. J. Neurophysiol. 86, 1095–1103.
Thompson, R.J., Zhou, N., MacVicar, B.A., 2006. Ischemia opens neuronal gap junction hemichannels. Science 312, 924–927.
Trapp, S., Ballanyi, K., 1995. KATP channel mediation of anoxia-induced outward current in rat dorsal vagal neurons in vitro. J. Physiol. 487 (Pt 1), 37–50.
Vanselow, B.K., Keller, B.U., 2000. Calcium dynamics and buffering in oculomotor neurones from mouse that are particularly resistant during amyotrophic lateral sclerosis (ALS)-related motoneurone disease. J. Physiol. 525 (Pt 2), 433–445.
Viana, F., Bayliss, D.A., Berger, A.J., 1994. Postnatal changes in rat hypoglossal motoneuron membrane properties. Neuroscience 59, 131–148.
von Lewinski, F., Keller, B.U., 2005. Ca^{2+}, mitochondria and selective motoneuron vulnerability: implications for ALS. Trends Neurosci. 28, 494–500.
Ye, J.H., Zhang, J., Xiao, C., Kong, J.Q., 2006. Patch-clamp studies in the CNS illustrate a simple new method for obtaining viable neurons in rat brain slices: glycerol replacement of NaCl protects CNS neurons. J. Neurosci. Methods 158, 251–259.
Yee, B.K., Balic, E., Singer, P., Schwerdel, C., Grampp, T., Gabernet, L., Knuesel, I., Benke, D., Feldon, J., Mohler, H., Boison, D., 2006. Disruption of glycine transporter 1 restricted to forebrain neurons is associated with a procognitive and antipsychotic phenotypic profile. J. Neurosci. 26, 3169–3181.